Object of Research

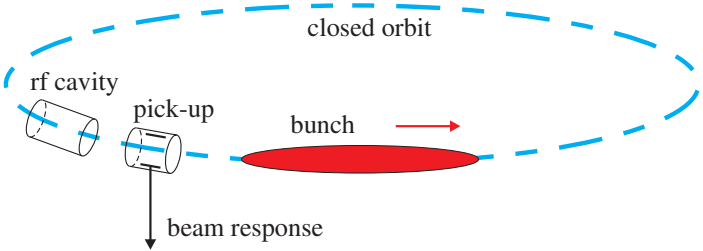

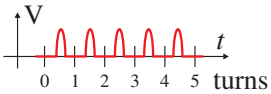

Object of Research

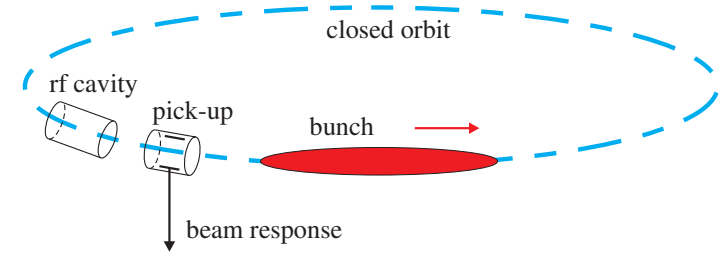

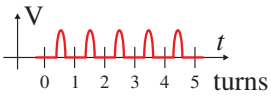

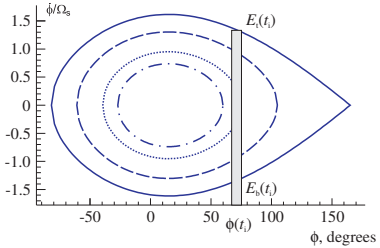

Object of Research

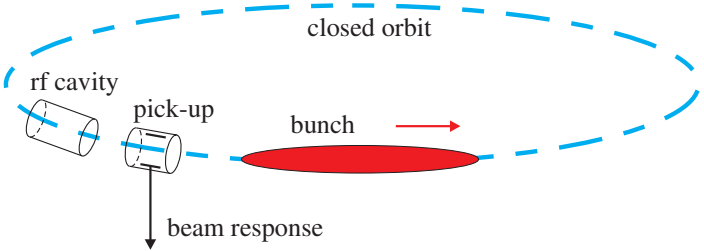

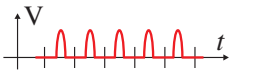

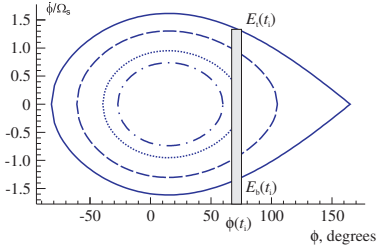

$\Rightarrow$

Longitudinal RMS parameters:

$$\sigma_t$$

$$\sigma_E$$

$$\varepsilon_s = \pi \sigma_t \sigma_E E_u$$

Phase space density:

$$I_\phi = N/(4\varepsilon_s)$$

Tomography

Tomography (Ancient Greek: tomos = “slice, section").
– destructive
– non-destructive (X-rays or Röntgen rays, **1895**)

Tomography

Tomography (Ancient Greek: tomos = “slice, section").
– destructive
– non-destructive (X-rays or Röntgen rays, **1895**)

Tomographic reconstruction is a type of multidimensional inverse problem where the challenge is to yield an estimate of a specific system from a finite number of projections.

1917: The Radon Transform is the mathematical basis for tomographic imaging that was laid down by the Austrian mathematician Johann Radon.

1979 Nobel Prize in Medicine: G. Hounsfield (English electrical engineer) and A. Cormac (South African American physicist) for works on X-ray computed tomography.

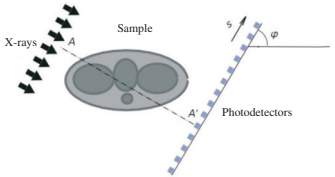

Tomography at accelerators

Phase Space Tomography: Steve Hancock and Mats Lindroos, CERN

1997–2004: based on the **A**lgebraic **R**econstruction **T**echnique (R.Gordon, 1974)

iterative algorithm for reconstruction an image from a series of angular projections

Tomographic measurements of longitudinal phase space density
S.Hancock, P.Knaus, M.Lindroos. EPAC98, Stockholm, Sweden. June 1998

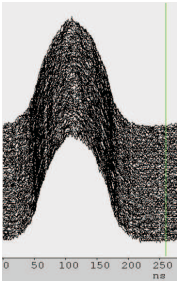

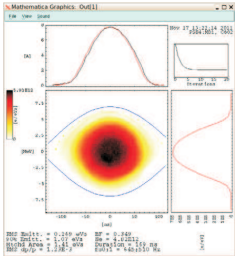

The turn-by-turn intensity profiles of a bunch rotating in longitudinal phase space are measured.
The method fully takes into account the non-linearities of particles' synchrotron motion.

Tomography at accelerators

Phase Space Tomography: Steve Hancock and Mats Lindroos, CERN

1997–2004: based on the **A**lgebraic **R**econstruction **T**echnique (R.Gordon, 1974)

iterative algorithm for reconstruction an image from a series of angular projections

Tomographic measurements of longitudinal phase space density
S.Hancock, P.Knaus, M.Lindroos. EPAC98, Stockholm, Sweden. June 1998

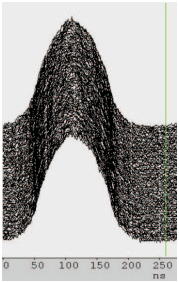

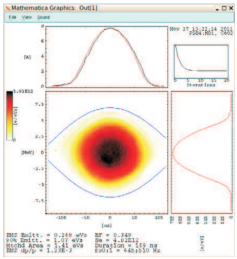

The turn-by-turn intensity profiles of a bunch rotating in longitudinal phase space are measured.
The method fully takes into account the non-linearities of particles' synchrotron motion.

Parameters of the tomographic reconstruction procedure **ART**: m, q, R_0, B, $\dot{B}$, V_{rf}, $\dot{V}_{\mathrm{rf}}$, h_{rf}, ρ, γ_{tr}.

Fundamentals of Synchrotron Acceleration

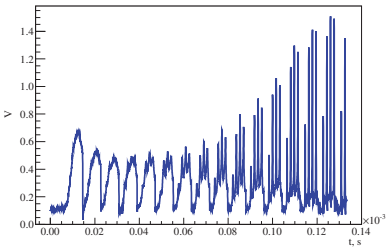

Signal of circulating bunches from pick-up

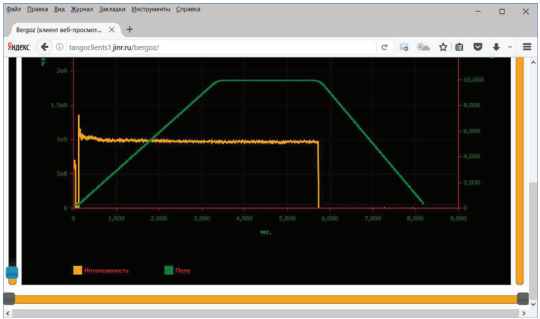

$N(t)$ (yellow) and $B(t)$ (green)

Fundamentals of Synchrotron Acceleration

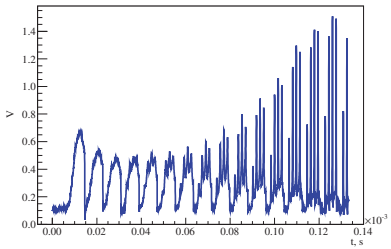

Signal of circulating bunches from pick-up

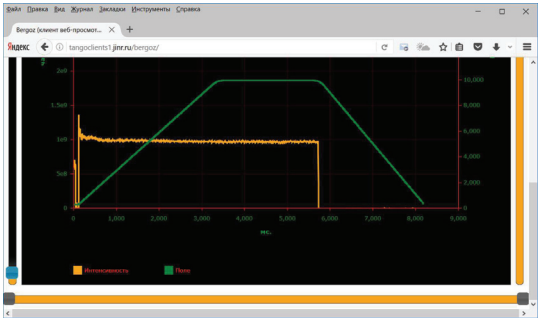

$N(t)$ (yellow) and $B(t)$ (green)

V. I. Veksler
1907 – 1966

- resonance condition for $\omega_{\mathrm{rf}}(B, R_0 = \mathrm{const}) \quad \Rightarrow$ accelerated particles

Fundamentals of Synchrotron Acceleration

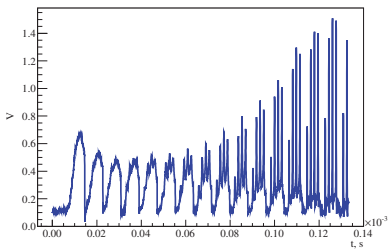

Signal of circulating bunches from pick-up

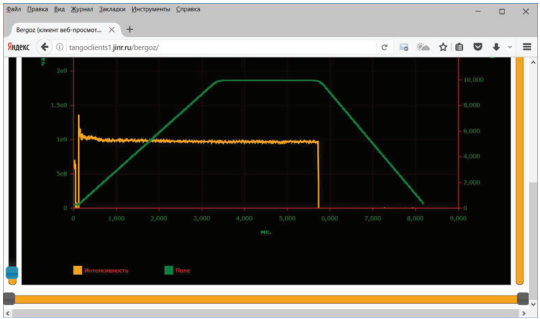

$N(t)$ (yellow) and $B(t)$ (green)

V. I. Veksler
1907 – 1966

- resonance condition for $\omega_{\mathrm{rf}}(B, R_0 = \mathrm{const}) \quad \Rightarrow$ accelerated particles
- longitudinal focusing $\Rightarrow$ a significant number of accelerated particles

Fundamentals of Synchrotron Acceleration

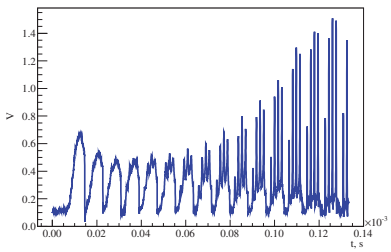

Signal of circulating bunches from pick-up

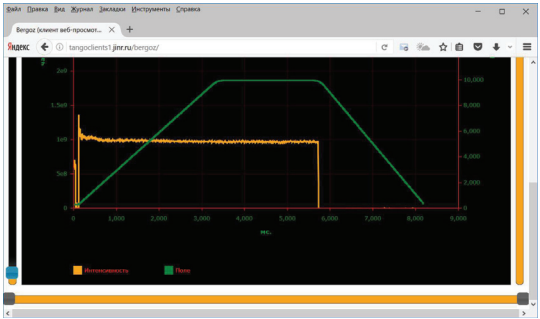

$N(t)$ (yellow) and $B(t)$ (green)

V. I. Veksler
1907 – 1966

- resonance condition for $\omega_{\mathrm{rf}}(B, R_0 = \mathrm{const}) \quad \Rightarrow$ accelerated particles
- longitudinal focusing $\Rightarrow$ a significant number of accelerated particles
- synchrotron motion equations $\Rightarrow$ the basis for tomography

Functional diagram to obtain the profile data

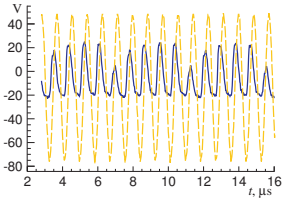

rf (yellow) and beam (blue) signals

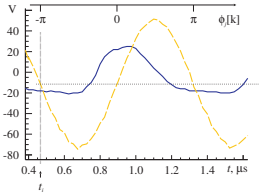

rf (yellow) and bunch (blue) signals

Functional diagram to obtain the profile data

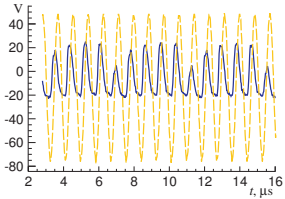

rf (yellow) and beam (blue) signals

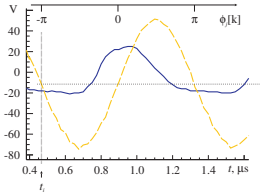

rf (yellow) and bunch (blue) signals

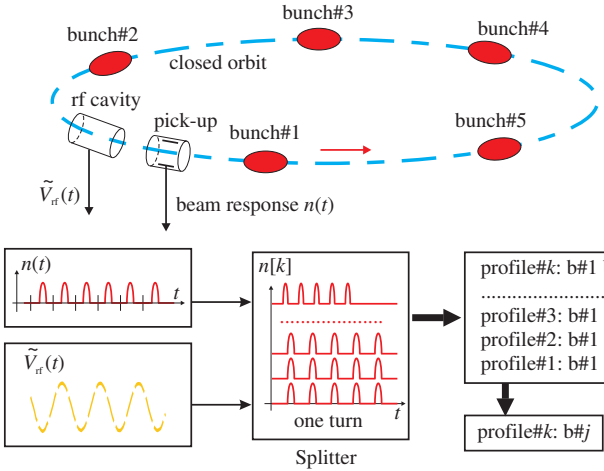

Zhabitsky V. M., Tomography of the Ion Bunches at the Nuclotron, XII International Scientific Workshop in Memory of V. P. Sarantsev, 5 – 8 September 2017, Alushta, Russia, http://sarantsev17.jinr.ru

Deuterons, D, 22.12.2016 18:46:38, $h_{\mathrm{rf}} = 5$, $\Delta t = 50$ ms

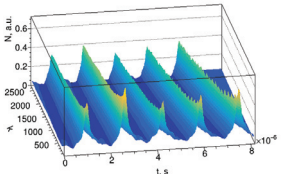

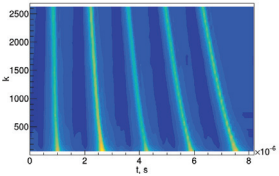

7653 turns

Deuterons, D, 22.12.2016 18:46:38, $h_{\mathrm{rf}} = 5$, $\Delta t = 50$ ms

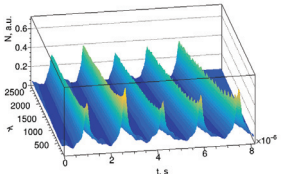

7653 turns

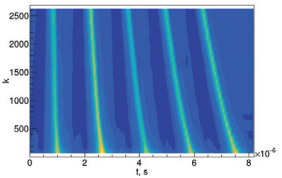

Profile Data for fragment:

- $\dot{B} = \mathrm{const}$
- $V_{\mathrm{rf}} = \mathrm{const}$

$\Rightarrow$ bunch #1, $t_{\mathrm{init}} = 42$ ms

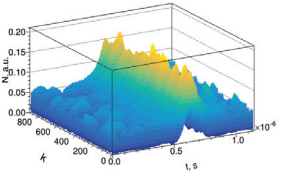

Deuterons, D, 22.12.2016 18:46:38, $h_{\mathrm{rf}} = 5$, $\Delta t = 50$ ms

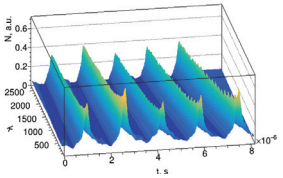

7653 turns

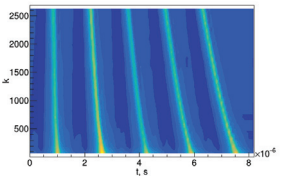

Profile Data for fragment:

- $\dot{B} = \mathrm{const}$
- $V_{\mathrm{rf}} = \mathrm{const}$

$\Rightarrow$ bunch #1, $t_{\mathrm{init}} = 42$ ms

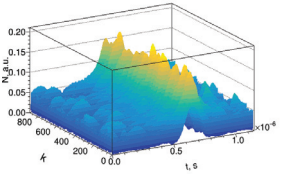

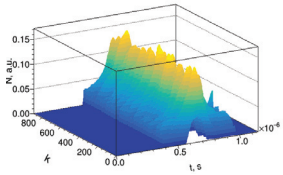

$\kappa_{\mathrm{m}} = 0.9$

Deuterons, D, 22.12.2016 18:46:38, $h_{\mathrm{rf}} = 5$, $\Delta t = 50$ ms

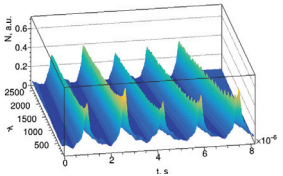

7653 turns

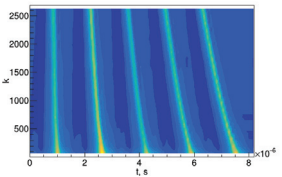

Profile Data for fragment:

- $\dot{B} = \mathrm{const}$
- $V_{\mathrm{rf}} = \mathrm{const}$

$\Rightarrow$ bunch #1, $t_{\mathrm{init}} = 42$ ms

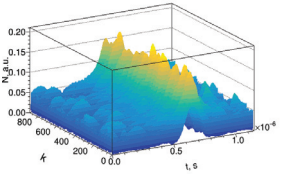

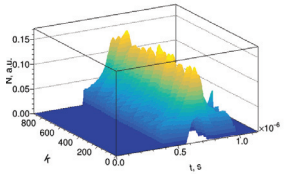

$\kappa_{\mathrm{m}} = 0.9$

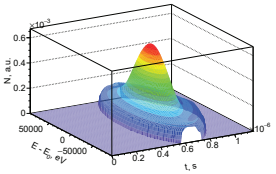

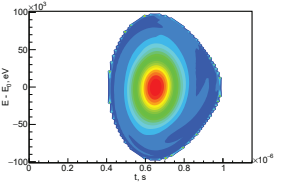

Deuterons, D, 22.12.2016 18:46:38, $h_{\mathrm{rf}} = 5$, $\Delta t = 50$ ms

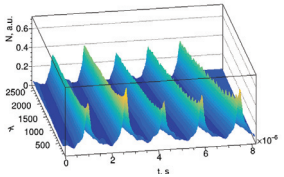

7653 turns

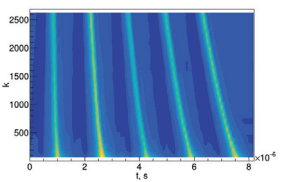

Profile Data for fragment:

- $\dot{B} = \mathrm{const}$
- $V_{\mathrm{rf}} = \mathrm{const}$

$\Rightarrow$ bunch #1, $t_{\mathrm{init}} = 42$ ms

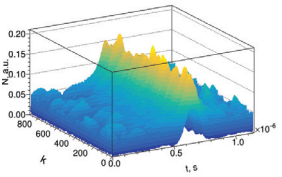

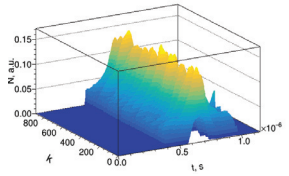

$\kappa_{\mathrm{m}} = 0.9$

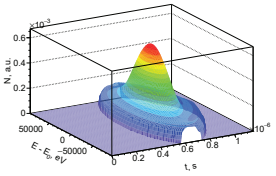

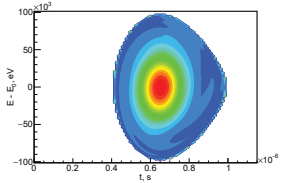

Requirements for tomographic reconstruction:

- $N_{\mathrm{bunch}}(t)$, $\tilde{V}_{\mathrm{rf}}(t)$
- m, q, R_0, B, $\dot{B}$, V_{rf}, $\dot{V}_{\mathrm{rf}}$, h_{rf}, ρ, γ_{tr}.

Testing of tomographic reconstruction: theoretical model for a bunch

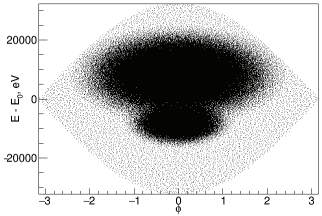

Distribution of ions in the bunch ($\dot{B} = \dot{V} = 0$)

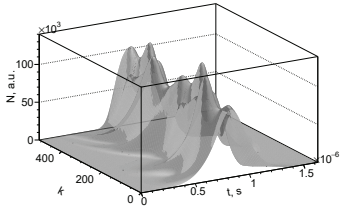

Profile data

Testing of tomographic reconstruction: theoretical model for a bunch

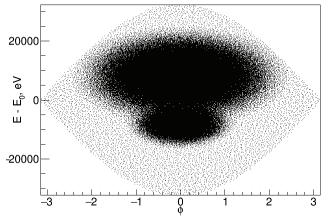

Distribution of ions in the bunch ($\dot{B} = \dot{V} = 0$)

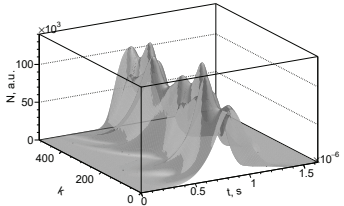

Profile data

Result of tomographic reconstruction (basic procedure):

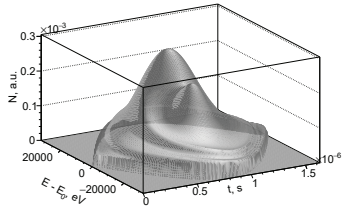

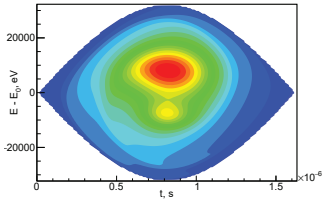

Testing of tomographic reconstruction

Piecewise-defined functions without jumps of its first and second derivatives are used for definition of:

- magnetic cycle $B(t)$

$$\text{for } t \in [t_i, t_{i+1}]: \qquad B(t) = B(t_i) + \dot{B}(t_i)(t - t_i) + \frac{1}{6}\dddot{B}(t_i)(t - t_i)^3 + \frac{1}{24}\ddddot{B}(t_i)(t - t_i)^4$$

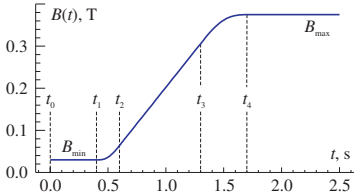

magnetic field $B(t)$

Cheblakov P., Derbenev A., Kadyrov R. et al. NSLS-II Booster Ramp Handling
Proc. of the 14th International Conference on Accelerator & Large Experimental Physics Control Systems ICALEPCS2013, 6–11 October 2013, San Francisco, USA. NIF/LLNL, JACoW.org, 2013. Pp. 1189–1192.

Testing of tomographic reconstruction

Piecewise-defined functions without jumps of its first and second derivatives are used for definition of:

- magnetic cycle $B(t)$

  for $t \in [t_i, t_{i+1}]$: $\quad B(t) = B(t_i) + \dot{B}(t_i)(t - t_i) + \frac{1}{6}\dddot{B}(t_i)(t - t_i)^3 + \frac{1}{24}\ddddot{B}(t_i)(t - t_i)^4$

- accelerating field $\tilde{V}_{\mathrm{rf}}(t) = V(t)\cos(\omega_{\mathrm{rf}}(t) + \varphi_0)$

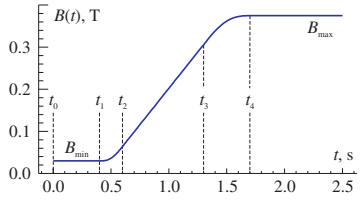

magnetic field $B(t)$

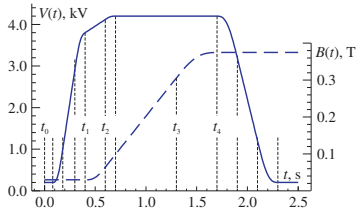

amplitude rf curve $V(t)$

Cheblakov P., Derbenev A., Kadyrov R. et al. NSLS-II Booster Ramp Handling
Proc. of the 14th International Conference on Accelerator & Large Experimental Physics Control Systems ICALEPCS2013, 6–11 October 2013, San Francisco, USA. NIF/LLNL, JACoW.org, 2013. Pp. 1189–1192.

Testing of tomographic reconstruction

Piecewise-defined functions without jumps of its first and second derivatives are used for definition of:

- magnetic cycle $B(t)$

  for $t \in [t_i, t_{i+1}]$: $\quad B(t) = B(t_i) + \dot{B}(t_i)(t - t_i) + \frac{1}{6}\dddot{B}(t_i)(t - t_i)^3 + \frac{1}{24}\ddddot{B}(t_i)(t - t_i)^4$

- accelerating field $\tilde{V}_{\mathrm{rf}}(t) = V(t)\cos(\omega_{\mathrm{rf}}(t) + \varphi_0)$

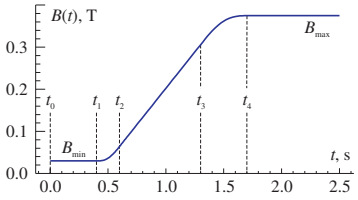

magnetic field $B(t)$

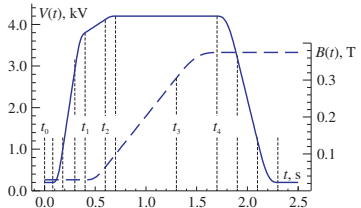

amplitude rf curve $V(t)$

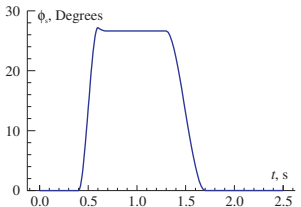

synchronus phase ϕ_s

Cheblakov P., Derbenev A., Kadyrov R. et al. NSLS-II Booster Ramp Handling
Proc. of the 14th International Conference on Accelerator & Large Experimental Physics Control Systems ICALEPCS2013, 6–11 October 2013, San Francisco, USA. NIF/LLNL, JACoW.org, 2013. Pp. 1189–1192.

Testing of tomographic reconstruction: theoretical model

$T_{\text{init}} = 5$ ms;
$\phi_s = 0°$
$W = 5$ MeV/u;

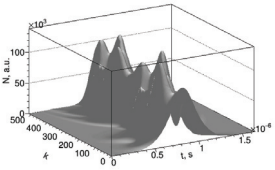

$T_{\text{init}} = 500$ ms;
$\phi_s = 11.4°$
7.4 MeV/u;

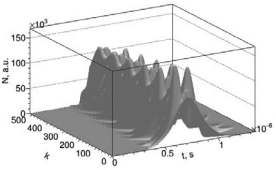

$T_{\text{init}} = 1$ s;
$\phi_s = 22.1°$
207.7 MeV/u;

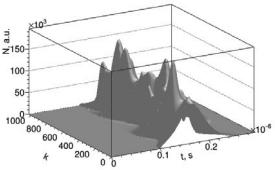

Testing of tomographic reconstruction: theoretical model

$T_{\text{init}} = 5$ ms;
$\phi_s = 0°$
$W = 5$ MeV/u;

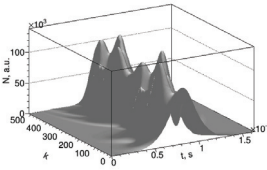

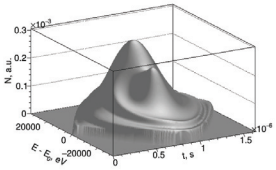

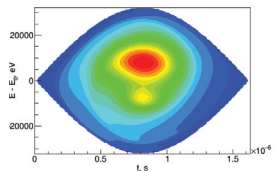

$T_{\text{init}} = 500$ ms;
$\phi_s = 11.4°$
7.4 MeV/u;

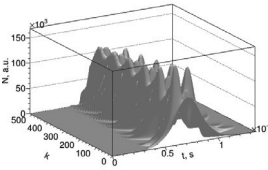

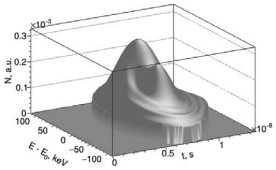

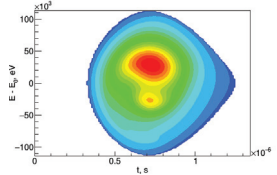

$T_{\text{init}} = 1$ s;
$\phi_s = 22.1°$
207.7 MeV/u;

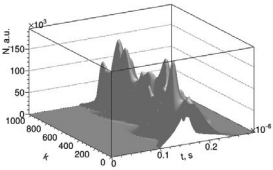

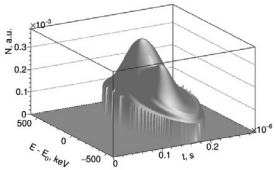

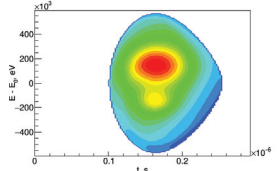

Carbon, C^{6+}, 16.03.2018 16:44:45, $h_{\mathrm{rf}} = 5$

Beam: $\Delta t = 800$ ms, 554640 turns

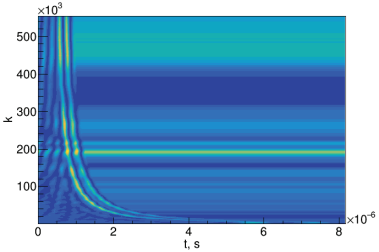

after injection: $\Delta t = 20$ ms, 2452 turns

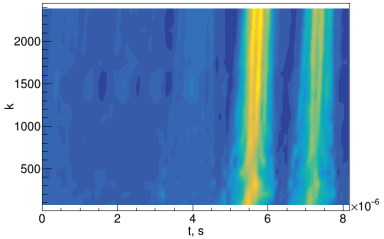

Carbon, C^{6+}, 16.03.2018 16:44:45, $h_{\mathrm{rf}} = 5$

Beam: $\Delta t = 800$ ms, 554640 turns

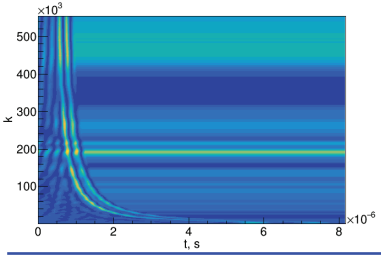

after injection: $\Delta t = 20$ ms, 2452 turns

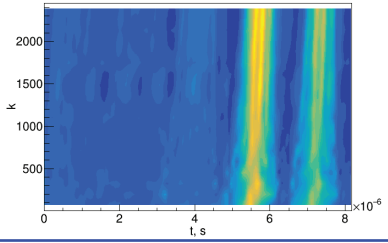

Bunch #4

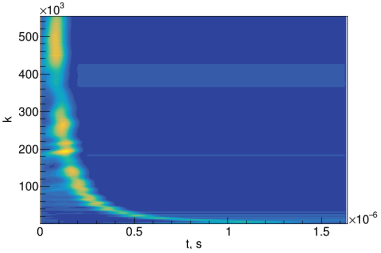

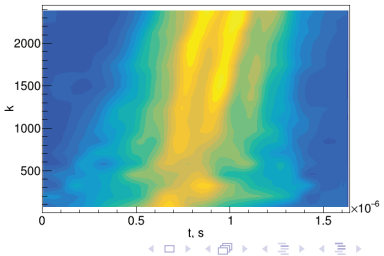

Fitting of $B(t)$: Carbon, C^{6+}, 16.03.2018 16:44:45

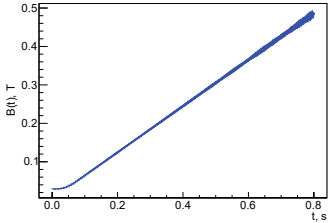

$B(t)$ calculated from $f_{\mathrm{rev}}(t)$
(554641 turns)

Fitting of $B(t)$: Carbon, C^{6+}, 16.03.2018 16:44:45

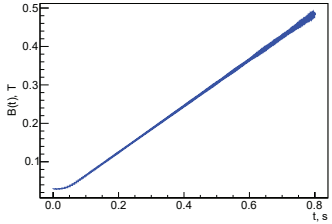

$B(t)$ calculated from $f_{\text{rev}}(t)$
(554641 turns)

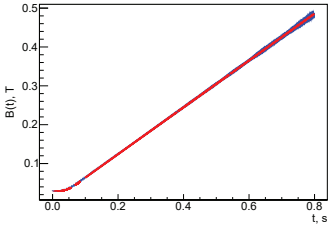

$B(t)$ fitted by polynomials

$B(t)$	t_1, ms	t_r, ms	N_{rev}
pol0	0.002	0.795	97
pol4	3.008	11.998	1101
pol4	12.308	59.997	6454
pol4	70.002	85.997	3298
pol4	100.000	380.000	150689
pol4	383.000	539.999	131648
pol1	543.000	799.997	250886

Fitting of $B(t)$: Carbon, C^{6+}, 16.03.2018 16:44:45

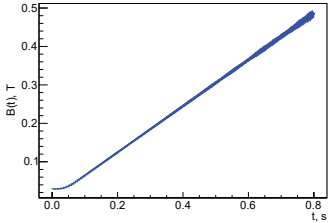

$B(t)$ calculated from $f_{\mathrm{rev}}(t)$
(554641 turns)

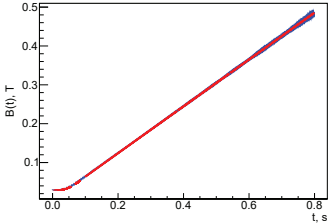

$B(t)$ fitted by polynomials

$B(t)$	t_1, ms	t_r, ms	N_{rev}
pol0	0.002	0.795	97
pol4	3.008	11.998	1101
pol4	12.308	59.997	6454
pol4	70.002	85.997	3298
pol4	100.000	380.000	150689
pol4	383.000	539.999	131648
pol1	543.000	799.997	250886

$B(t)$	t_1, ms
pol0	0.002
pol4	9.000
pol4	13.593
pol4	64.704
pol4	94.504
pol4	381.104
pol1	552.389

Fitting of $B(t)$: Carbon, C^{6+}, 16.03.2018 16:44:45

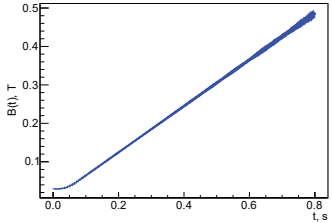

$B(t)$ calculated from $f_{\mathrm{rev}}(t)$
(554641 turns)

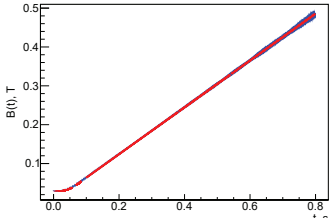

$B(t)$ fitted by polynomials

$B(t)$	t_1, ms	t_r, ms	N_{rev}
pol0	0.002	0.795	97
pol4	3.008	11.998	1101
pol4	12.308	59.997	6454
pol4	70.002	85.997	3298
pol4	100.000	380.000	150689
pol4	383.000	539.999	131648
pol1	543.000	799.997	250886

$B(t)$	t_1, ms
pol0	0.002
pol4	9.000
pol4	13.593
pol4	64.704
pol4	94.504
pol4	381.104
pol1	552.389

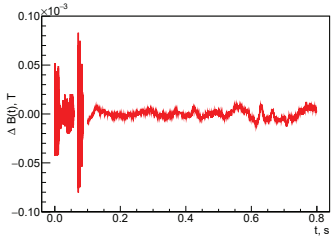

$< \Delta B(t) >$

Fitting of $B(t)$: Carbon, C^{6+}, 16.03.2018 16:44:45

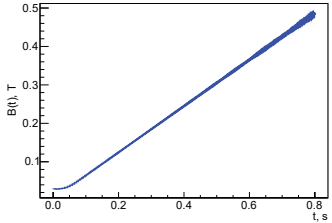

$B(t)$ calculated from $f_{\mathrm{rev}}(t)$
(554641 turns)

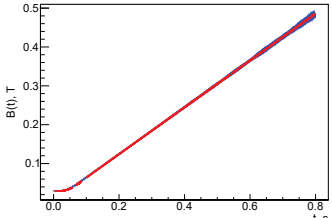

$B(t)$ fitted by polynomials

$B(t)$	t_1, ms	t_r, ms	N_{rev}
pol0	0.002	0.795	97
pol4	3.008	11.998	1101
pol4	12.308	59.997	6454
pol4	70.002	85.997	3298
pol4	100.000	380.000	150689
pol4	383.000	539.999	131648
pol1	543.000	799.997	250886

$B(t)$	t_1, ms
pol0	0.002
pol4	9.000
pol4	13.593
pol4	64.704
pol4	94.504
pol4	381.104
pol1	552.389

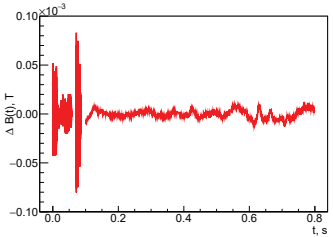

$< \Delta B(t) >$

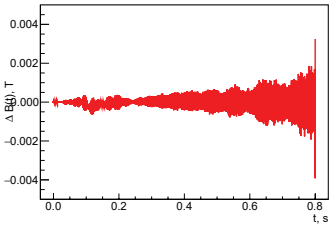

$\Delta B(t)$

Results from polynomials

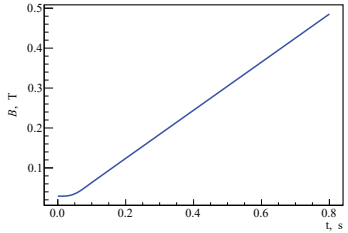

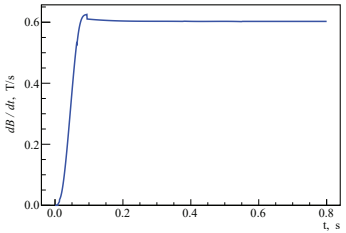

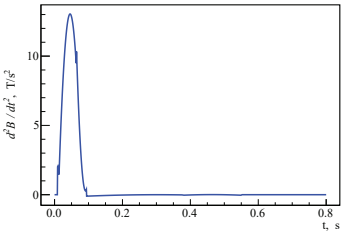

Fitting of $V(t)$: 23.03.2018 16:36

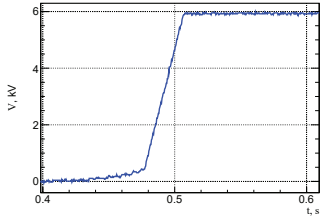

$V(t)$ from accelerating gap

$$\dot{V}(t = 0.5\,\text{s}) \approx 187\ \text{kV/s}$$

Bunch #4

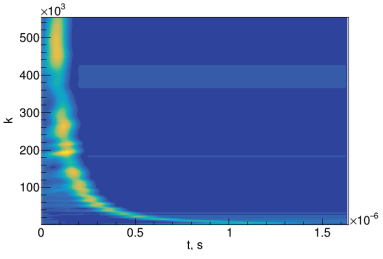

Profile Data:

$500\,\text{ms} < t < 501\,\text{ms}$, $\kappa_\text{m} = 0.9$

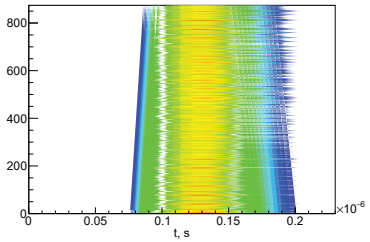

Bunch #4

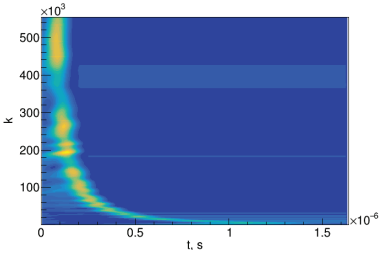

Profile Data:

$500\,\text{ms} < t < 501\,\text{ms}$, $\kappa_\text{m} = 0.9$

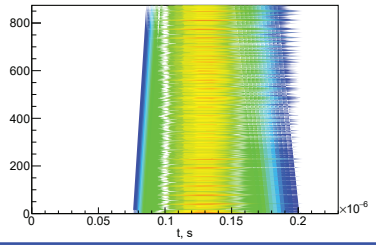

Distribution of ions:

$t_\text{init} = 500\,\text{ms}$

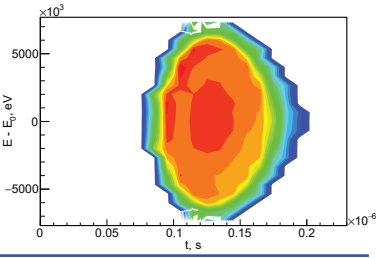

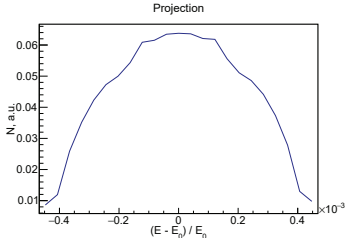

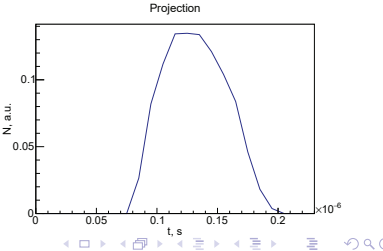

Film start (bunch #4): 500 ms after injection (step: 21 turns, 7 slides)

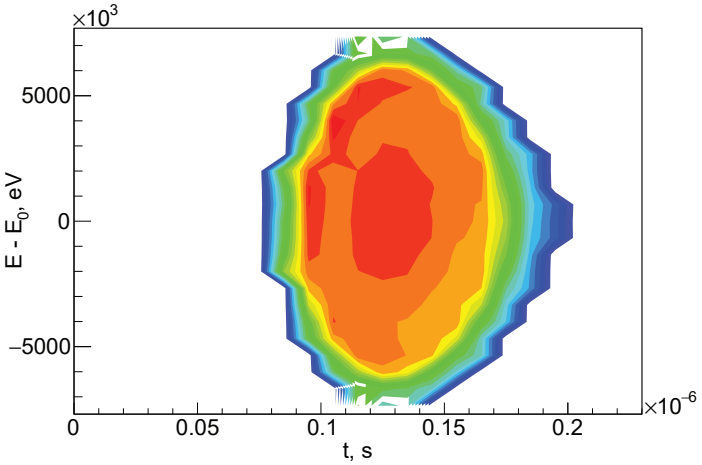

Film start (bunch #4): 500 ms after injection (step: 21 turns, 7 slides)

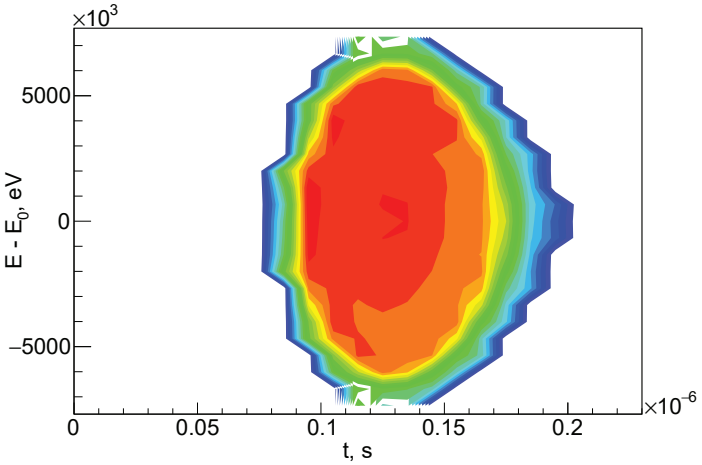

Film start (bunch #4): 500 ms after injection (step: 21 turns, 7 slides)

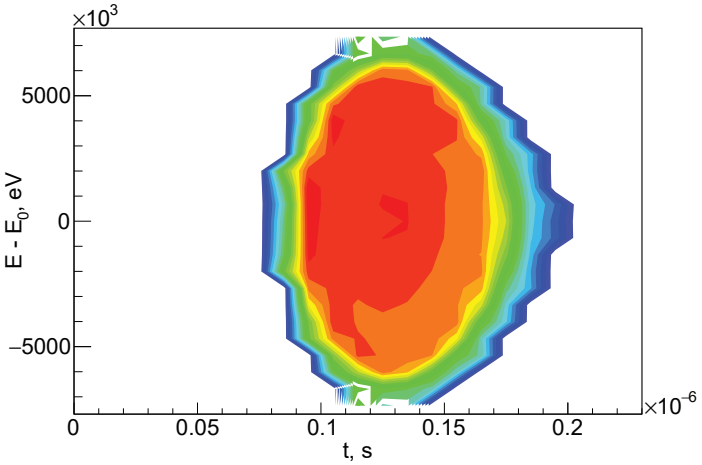

Film start (bunch #4): 500 ms after injection (step: 21 turns, 7 slides)

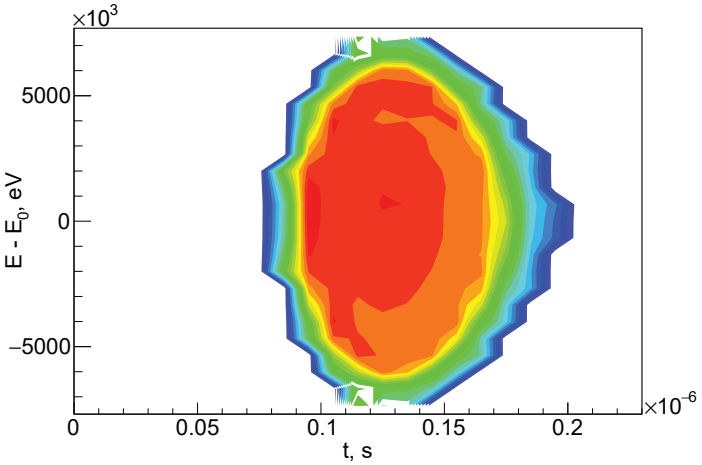

Film start (bunch #4): 500 ms after injection (step: 21 turns, 7 slides)

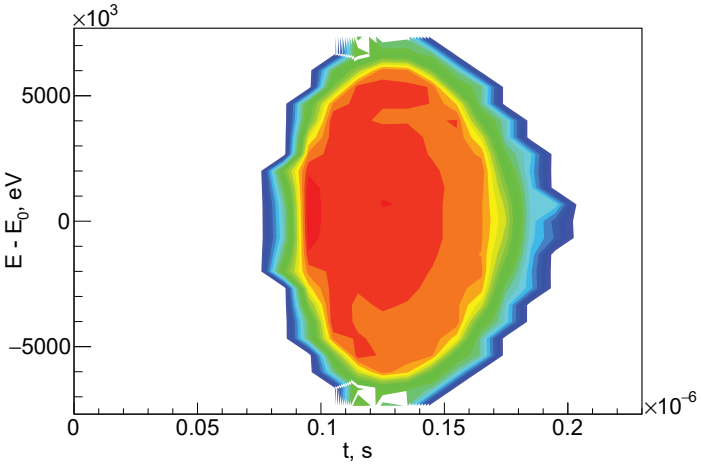

Film start (bunch #4): 500 ms after injection (step: 21 turns, 7 slides)

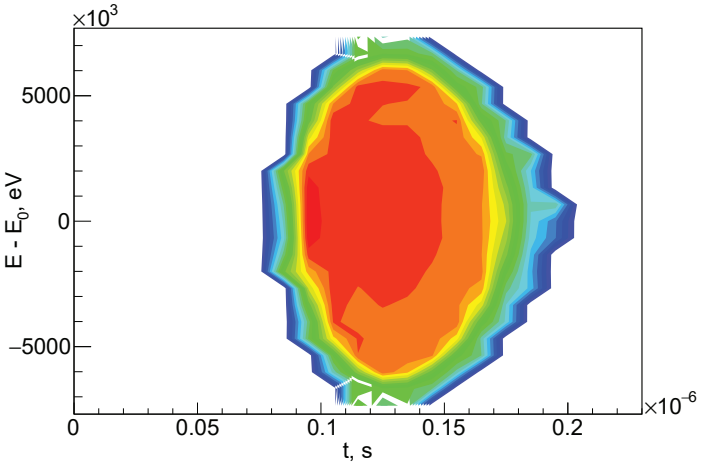

Film start (bunch #4): 500 ms after injection (step: 21 turns, 7 slides)

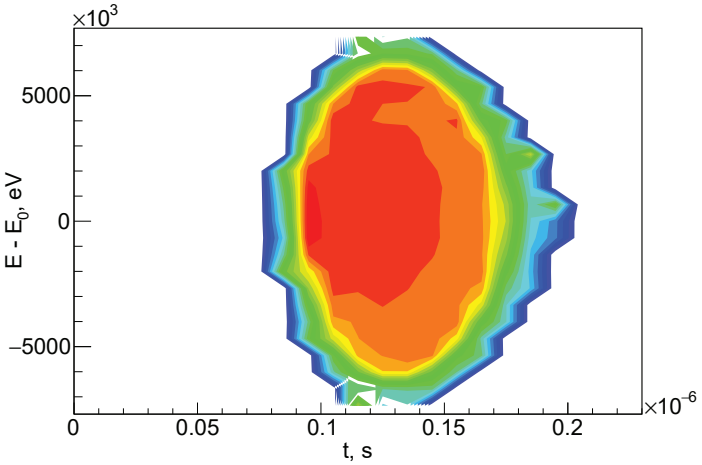

Profile Data:

$1\,\text{ms} < t < 6\,\text{ms}$, $\kappa_\text{m} = 0.9$

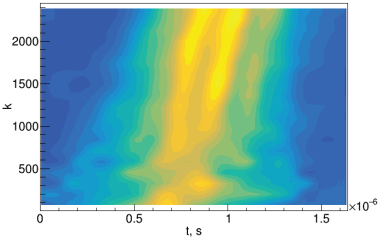

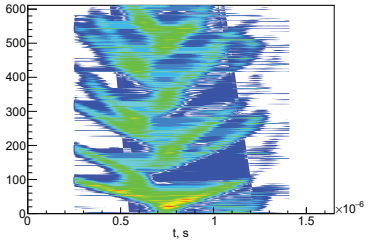

Carbon, C^{6+}, 16.03.2018 16:44:45, Bunch #4

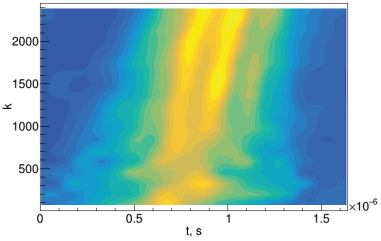

Profile Data:

$1\ \text{ms} < t < 6\ \text{ms},\ \kappa_{\text{m}} = 0.9$

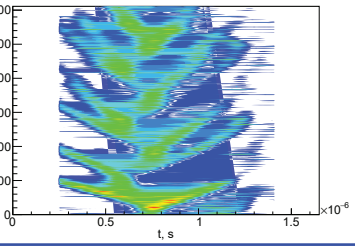

Distribution of ions:

$t_{\text{init}} = 1\ \text{ms}$

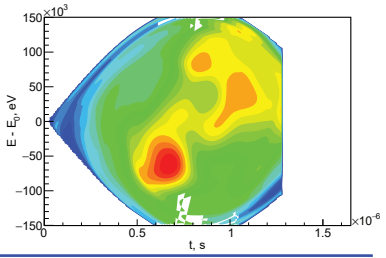

Projection

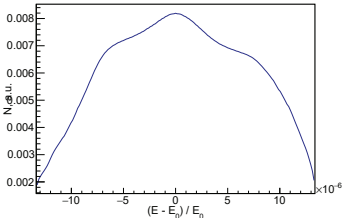

Projection

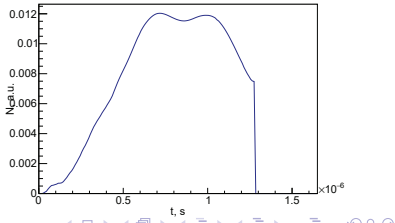

Film start (bunch #4): 1 ms after injection (step: 21 turns, 6 slides)

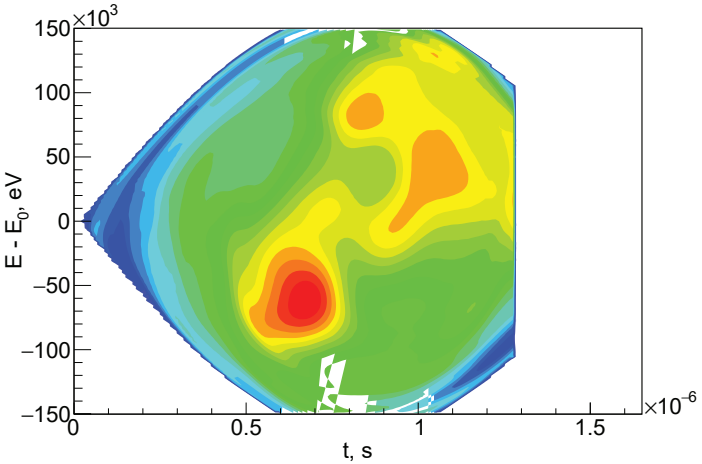

Film start (bunch #4): 1 ms after injection (step: 21 turns, 6 slides)

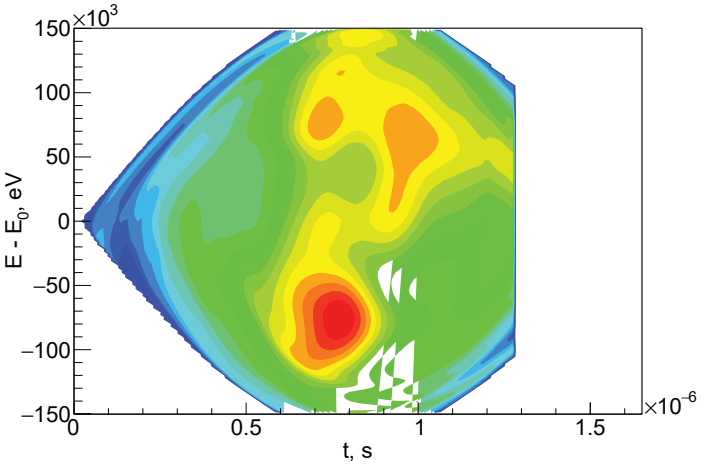

Film start (bunch #4): 1 ms after injection (step: 21 turns, 6 slides)

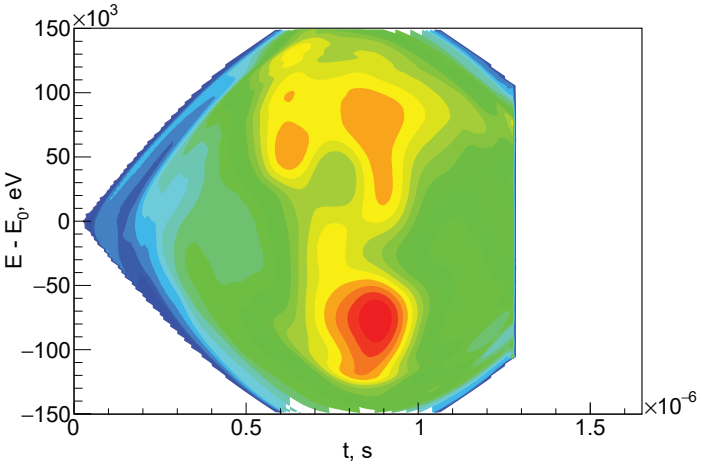

Film start (bunch #4): 1 ms after injection (step: 21 turns, 6 slides)

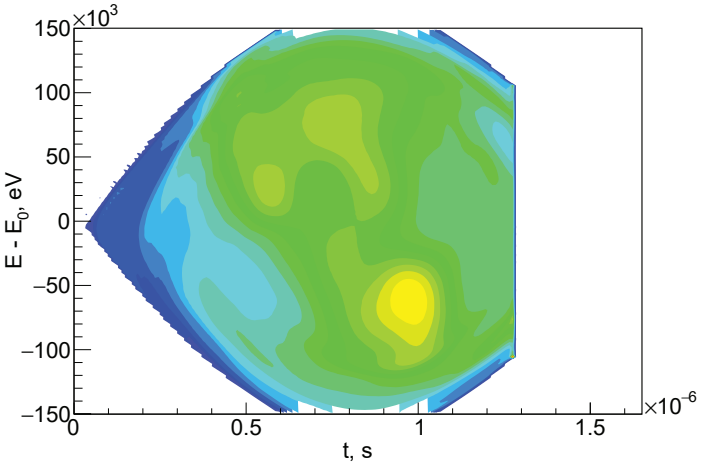

Film start (bunch #4): 1 ms after injection (step: 21 turns, 6 slides)

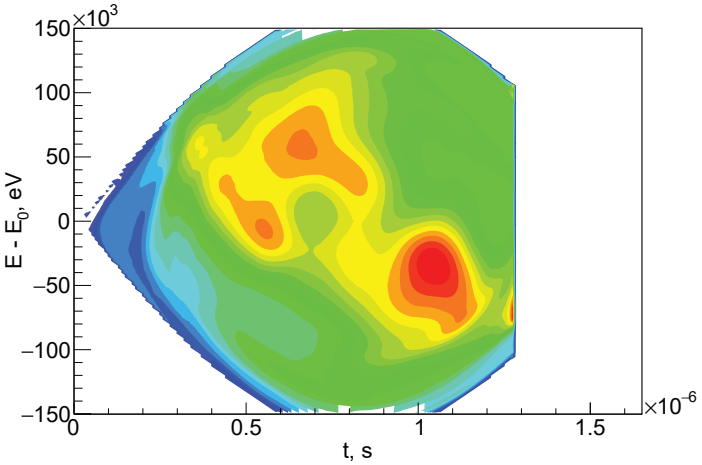

Film start (bunch #4): 1 ms after injection (step: 21 turns, 6 slides)

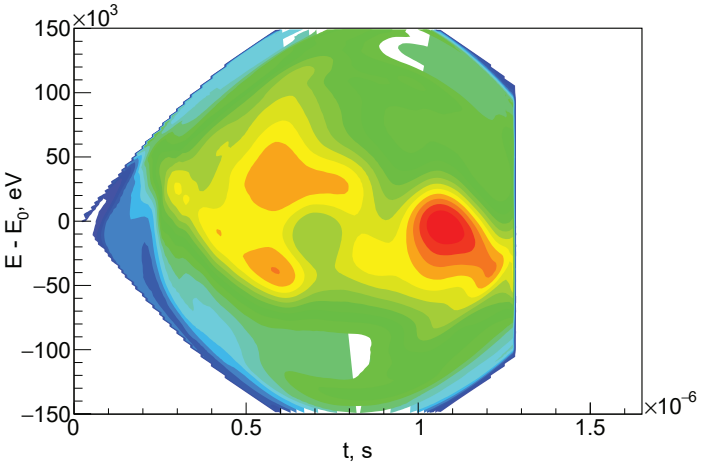

Longitudinal Phase Space Tomography at the Nuclotron

Beam: Li^{3+}, Date: 23.03.2017 17:40:50
Bunches #1 - #5 after injection ($\Delta t = 10$ ms)

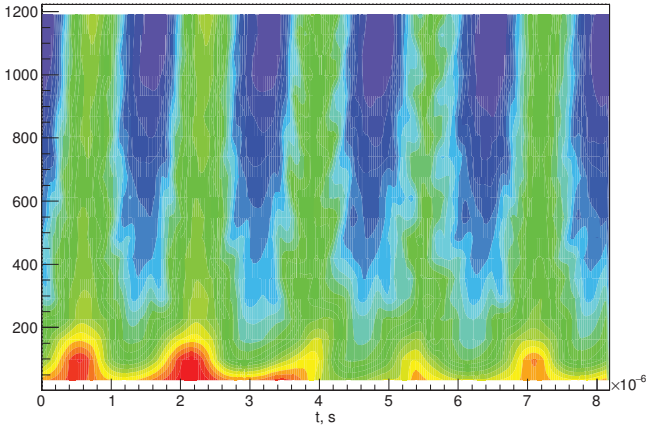

Longitudinal Phase Space Tomography at the Nuclotron

Beam: Li^{3+}, Date: 23.03.2017 17:40:50
Film start (bunch #2): 5 ms after injection (step: 14 turns; 11 slides)

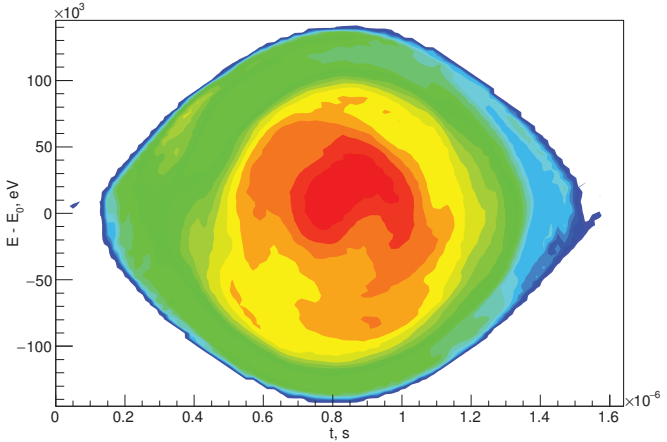

Longitudinal Phase Space Tomography at the Nuclotron

Beam: Li^{3+}, Date: 23.03.2017 17:40:50
Film start (bunch #2): 5 ms after injection (step: 14 turns; 11 slides)

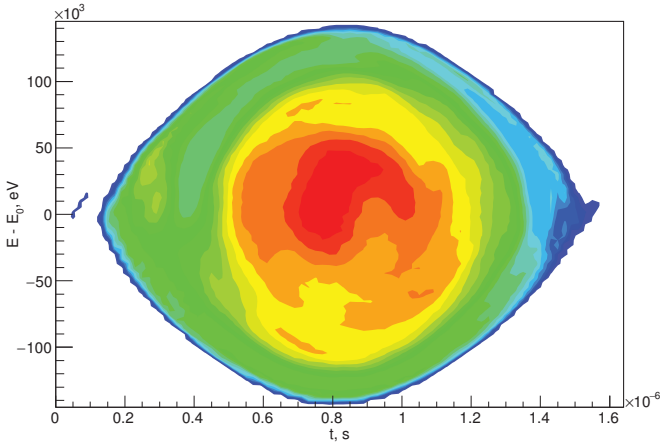

Longitudinal Phase Space Tomography at the Nuclotron

Beam: Li^{3+}, Date: 23.03.2017 17:40:50
Film start (bunch #2): 5 ms after injection (step: 14 turns; 11 slides)

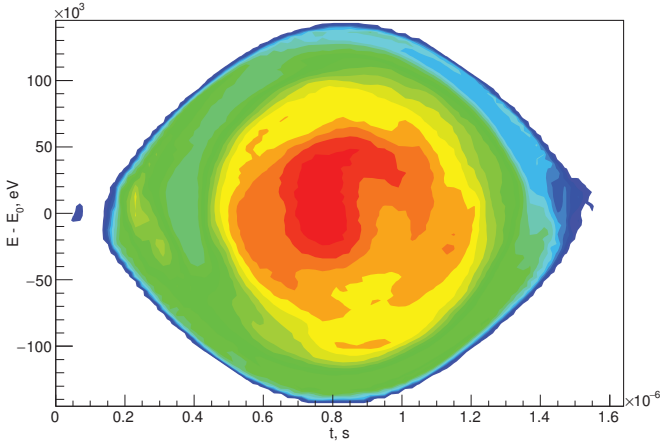

Longitudinal Phase Space Tomography at the Nuclotron

Beam: Li^{3+}, Date: 23.03.2017 17:40:50
Film start (bunch #2): 5 ms after injection (step: 14 turns; 11 slides)

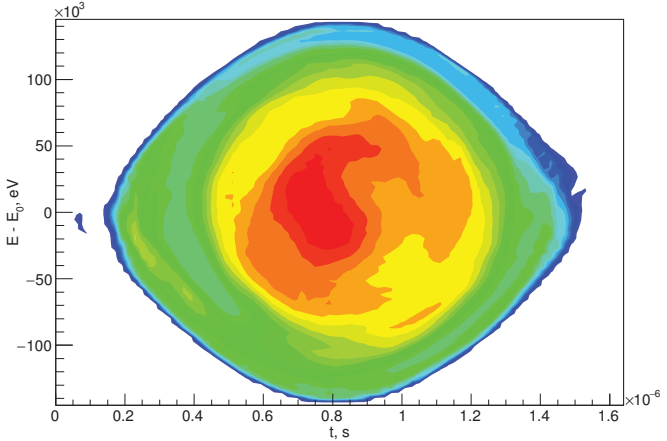

Longitudinal Phase Space Tomography at the Nuclotron

Beam: Li^{3+}, Date: 23.03.2017 17:40:50
Film start (bunch #2): 5 ms after injection (step: 14 turns; 11 slides)

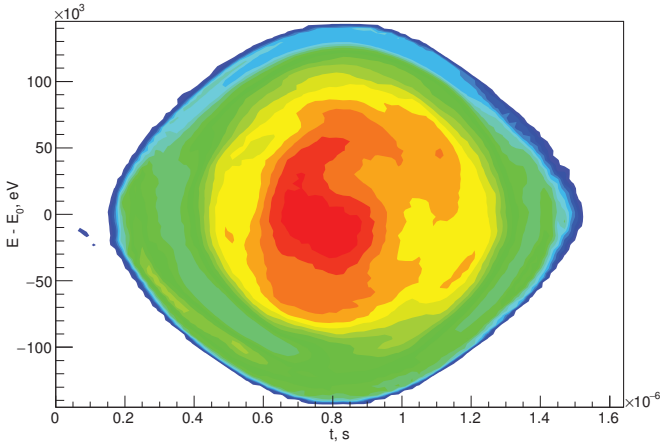

Longitudinal Phase Space Tomography at the Nuclotron

Beam: Li^{3+}, Date: 23.03.2017 17:40:50
Film start (bunch #2): 5 ms after injection (step: 14 turns; 11 slides)

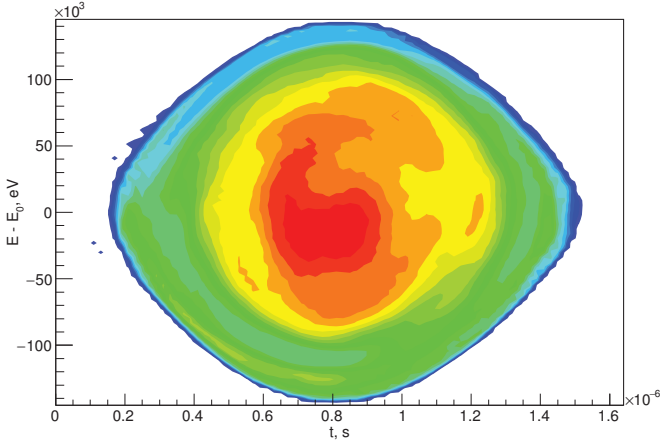

Longitudinal Phase Space Tomography at the Nuclotron

Beam: Li^{3+}, Date: 23.03.2017 17:40:50
Film start (bunch #2): 5 ms after injection (step: 14 turns; 11 slides)

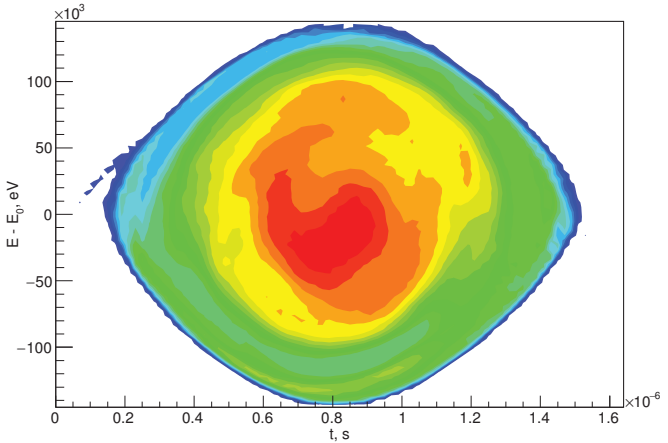

Longitudinal Phase Space Tomography at the Nuclotron

Beam: Li^{3+}, Date: 23.03.2017 17:40:50
Film start (bunch #2): 5 ms after injection (step: 14 turns; 11 slides)

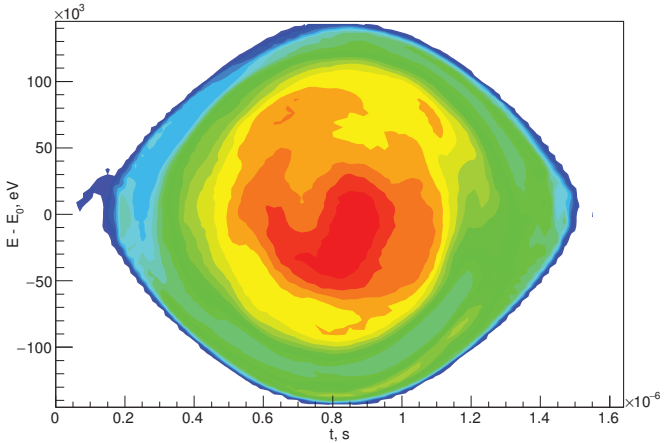

Longitudinal Phase Space Tomography at the Nuclotron

Beam: Li^{3+}, Date: 23.03.2017 17:40:50
Film start (bunch #2): 5 ms after injection (step: 14 turns; 11 slides)

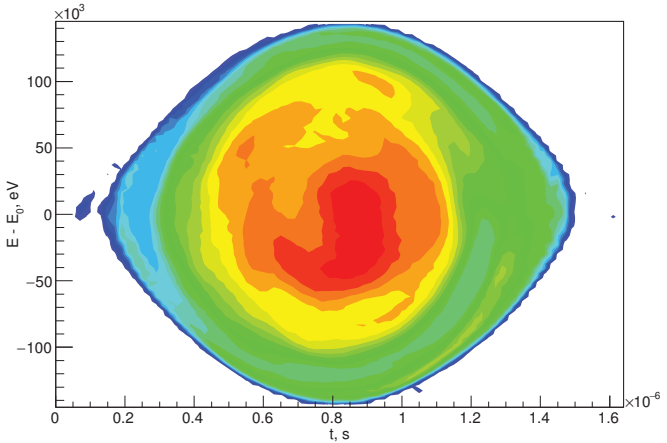

Longitudinal Phase Space Tomography at the Nuclotron

Beam: Li^{3+}, Date: 23.03.2017 17:40:50
Film start (bunch #2): 5 ms after injection (step: 14 turns; 11 slides)

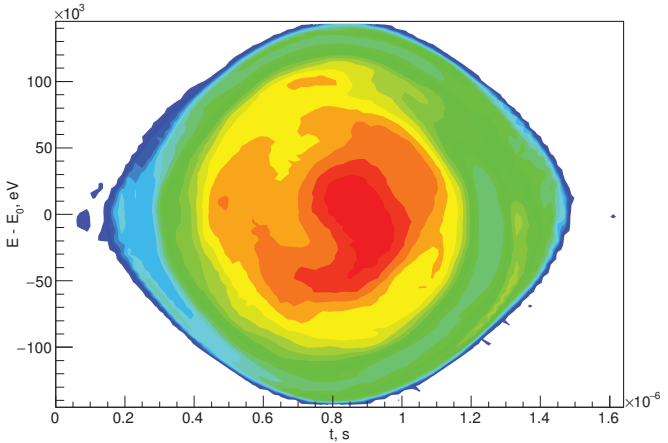

Longitudinal Phase Space Tomography at the Nuclotron

Beam: Li^{3+}, Date: 23.03.2017 17:40:50
Film start (bunch #2): 5 ms after injection (step: 14 turns; 11 slides)

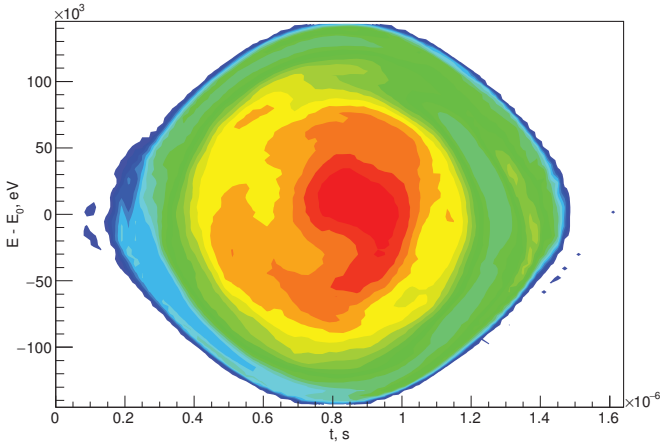

Conclusion

- Tomographic reconstruction of the longitudinal distribution function of ions in bunches during acceleration was successfully tested at the Nuclotron.
- The technique of B-fitting on the basis of experimental data on rf frequency was developed.
- Tomographic reconstruction procedure was improved for an arbitrary dependencies of $B(t)$ and $V(t)$ on time t.
- Computed procedure developed can be used for estimation of longitudinal parameters of ion bunches.

Conclusion

- Tomographic reconstruction of the longitudinal distribution function of ions in bunches during acceleration was successfully tested at the Nuclotron.
- The technique of B-fitting on the basis of experimental data on rf frequency was developed.
- Tomographic reconstruction procedure was improved for an arbitrary dependencies of $B(t)$ and $V(t)$ on time t.
- Computed procedure developed can be used for estimation of longitudinal parameters of ion bunches.

Acknowledgements
A. Butenko, E. Gorbachev, S. Romanov, O. Brovko, A. Grebentsov, V. Karpinsky, B. Vasilishin, V. Andreev, V. Slepnev (JINR)

Thank you for listening.